Nucleon transfer to continuum states

A. Bonaccorso
Istituto Nazionale di Fisica Nucleare, Sezioni di Catania e Pisa, 56100 Pisa, Italy

D. M. Brink
Department of Theoretical Physics, University of Oxford, Oxford OX1 3NP, United Kingdom
(Received 28 March 1988)

A semiclassical model is presented for the calculation of energy spectra of one nucleon transfer reactions to continuum states. Both isolated and overlapping resonances can be discussed. The theory is applied to medium energy heavy-ion reactions and the calculated spectra show general trends in agreement with the experimental data.

I. INTRODUCTION

In this paper we present a formalism for studying single nucleon transfer reactions between heavy ions when the final state of the transfered nucleon is in the continuum. It is a natural extension of the formalism developed in[1-5] for nucleon transfer between bound states.

Nuclear reactions at incident energies well above the Coulomb barrier can lead to highly excited residual nuclei and in the case of a transfer reaction the transferred nucleon can have a continuous energy spectrum. Many approaches to the problem of calculating the cross section for such a reaction have been developed.[6-12] They are all based on extensions of the distorted-wave Born approximation (DWBA) theory to the case of an unbound final state. The work of Huby *et al.*[9,10] is similar to ours since in both theories the final state for the unbound nucleon is represented by a scattering state with an appropriate normalization. Other approaches[6-8] are based on statistical compound nucleus theories. They require quite lengthy numerical calculations and do not determine the absolute normalization. McVoy and Nemes[13] proposed a simple model based on the plane wave Born approximation to calculate both transfer to continuum and breakup. However, they obtained only very qualitative results.

A formula for the probability of transfer of a single neutron from an initial bound state to a final unbound state is obtained in Sec. II of this paper and the case of an isolated resonance is considered in Sec. III. In both the present approach and the one of Huby *et al.* it is found that the transfer probability is proportional to $|\sin\delta_l|^2$ where δ_l is the phase shift of the scattering wave function of the transferred nucleon by the final nucleus. The analysis in Secs. II and III is made for the case where the final state of the transferred nucleon is represented by a single-particle wave function but it can be generalized to more complicated situations. We discuss this generalization in Sec. IV of this paper and find that the transfer probability is proportional to $|1-S_{00}|^2$ where S_{00} is the elastic part of the scattering matrix for scattering of the transferred neutron by the final nucleus. If we take the energy average of this result the transfer cross section can be expressed in terms of the neutron optical-model S matrix. Some numerical results are presented in Sec. V.

II. TRANSFER TO CONTINUUM STATES

We begin the derivation from a formula for the transfer amplitude given in Ref. 4. The neutron makes a transition from a single-particle state ψ_1 with orbital angular momentum l_1,m_1 and energy ε_1 in the first nucleus to a state ψ_2 with angular momentum l_2,m_2 and energy ε_2 in the final nucleus. The two nuclei pass each other on classical orbits and the transfer amplitude is written as a surface integral over a surface Σ between the two nuclei. The relative velocity of the centers of the two nuclei at the point of closest approach is v and the z axis is chosen parallel to v. The surface Σ is parallel to the z-y plane. At the point of closest approach the center of the first nucleus is at a distance d_1 from Σ and the distance of the center of the second nucleus is d_2. The distance of closest approach between the two centers is $R=d_1+d_2$.

There are many equivalent ways of writing an approximate formula for the transfer amplitude. We start from Eq. (3.4) of Ref. 4

$$A_{21}=\frac{i\hbar}{2\pi mv}\int_{-\infty}^{+\infty}dk_y(\eta^2+k_y^2)^{1/2}\times\bar{\psi}_2^*(d_2,k_y,k_2)\bar{\psi}_1(d_1,k_y,k_1)\ . \quad (2.1)$$

Here $\bar{\psi}_\alpha(d_\alpha,k_y,k_z)$ is the double Fourier transform of the coordinate space wave function $\psi_1(\psi_2)$ of the initial (final) nucleon bound-state wave function

$$\bar{\psi}(x,k_y,k_z)=\int\int dy\,dz\,e^{-i(yk_y+zk_z)}\psi(x,y,z)\ . \quad (2.2)$$

The quantity η in Eq. (2.1) is defined by

$$\eta^2=k_1^2+\gamma_1^2=k_2^2+\gamma_2^2\ , \quad (2.3)$$

where

$$\gamma_\alpha^2=-\frac{2m\varepsilon_\alpha}{\hbar^2}\quad\text{for }\alpha=1,2 \quad (2.4)$$

and $\hbar k_1$ and $\hbar k_2$ are the z components of the momentum of the transferred neutron relative to the first and second

nuclei. They are given by

$$\hbar k_1 = -\frac{(Q+\frac{1}{2}mv^2)}{v}, \quad \hbar k_2 = -\frac{(Q-\frac{1}{2}mv^2)}{v} , \tag{2.5}$$

where $Q=\varepsilon_1-\varepsilon_2$ is the Q value of the reaction. Equation (2.1) shows the dependence of the transfer amplitude on the momentum distribution in the initial and final nuclear states: $\bar{\psi}(d_1,k_y,k_1)$ is the amplitude for finding the nucleon from the first nucleus on the surface Σ with momentum components $(k_y,k_z)=(k_y,k_1)$ and $\bar{\psi}_2(d_2,k_y,k_2)$ is the corresponding amplitude for the nucleon in the second nucleus. The restrictions (2.5) on the z components of the momentum of the nucleon in the initial and final nuclei are a consequence of energy and momentum balance along the direction of relative motion as explained in Ref. 4.

For cases where the initial and final single neutron states ψ_1 and ψ_2 are bound states the wave functions on the surface Σ may be approximated by their asymptotic forms

$$\psi(\underline{r}) \simeq -Ci^l \gamma h_l^{(1)}(i\gamma r) Y_{lm}(\theta,\varphi) , \tag{2.6}$$

where $h_l^{(1)}$ are Hankel functions of complex argument defined in Ref. 19, p. 415. The double Fourier transform of Eq. (2.6) calculated according to Eq. (2.2) is

$$\bar{\psi}(x,k_y,k_z) = -C\frac{2\pi}{\gamma_x} e^{-\gamma_x |x|} Y_{lm}(\hat{\mathbf{k}}) , \tag{2.7}$$

where

$$\underline{k}=(i\gamma_x,k_y,k_z), \quad \hat{\underline{k}}=\frac{\underline{k}}{|\underline{k}|}$$
$$|\underline{k}| = \sqrt{\underline{k}^*\cdot\underline{k}} = (k_y^2+k_z^2-\gamma_x^2)^{1/2} = i\gamma \tag{2.8}$$

$$\gamma_x^2 = k_y^2+k_z^2+\gamma^2 \tag{2.9}$$

and γ is related to the bound state energy ε by Eq. (2.4). In Eq. (2.7) C is the asymptotic normalization constant of the state ψ_α. When the Fourier transform (2.7) is substituted into (2.1) the integral can be evaluated to give the transfer amplitude

$$A(l_2m_2,l_1m_1) = -4\pi i\frac{\hbar}{mv} C_2C_1 K_{m_1-m_2}(\eta R) \times Y_{l_1m_1}(\beta_1,\pi) Y^*_{l_2m_2}(\beta_2,0) , \tag{2.10}$$

where the complex angles β_α are related to the k_α in Eq. (2.5) by

$$\cos\beta_\alpha = -\frac{ik_\alpha}{\gamma_\alpha}, \quad \sin\beta_\alpha = \frac{\eta}{\gamma_\alpha} . \tag{2.11}$$

Now we generalize the above results to the case where the final state is a single-particle unbound state ψ_f with angular momentum (l_f,m_f) and energy $\varepsilon_f>0$. Equation (2.6) for the asymptotic form of the final wave function is replaced by the scattering wave function with appropriate boundary conditions

$$\psi_f(\underline{r}) \simeq C_f k_f \tfrac{1}{2} i[h_{l_f}^{(+)}(k_f r) - e^{-2i\delta_{l_f}} h_{l_f}^{(-)}(k_f r)] \times Y_{l_f m_f}(\theta,\varphi) , \tag{2.12}$$

where $h_l^{(\pm)}$ are Hankel functions of real argument which, according to Ref. 19, can also be written as $h_l^{(1)} = -ih_l^{(+)}$ and $h_l^{(2)} = ih_l^{(-)}$, with

$$k_f^2 = \frac{2m\varepsilon_f}{\hbar^2} . \tag{2.13}$$

When r is very large the radial part of Eq. (2.12) can also be written as

$$R_{l_f} = \frac{2N}{r}\sin(kr - \tfrac{1}{2}l_f\pi + \delta_{l_f}) , \tag{2.14}$$

where δ_{l_f} is the l_f-wave phase shift. The normalization constants C_f and N are related by $C_f = 2Ni^{l_f}\exp(i\delta_{l_f})$. We choose the normalization constant N so that the wave function R_{l_f} is normalized in a large box of radius $L \gg R$. Then

$$N^2\int_0^L R_{l_f}^2(r) r^2 dr \approx 4N^2\int_0^L \sin^2(kr - \tfrac{1}{2}l_f\pi + \delta_{l_f}) dr = 1$$

then

$$N^2 = \frac{1}{2L}, \quad |C_f|^2 = \frac{2}{L} . \tag{2.15}$$

We now wish to calculate the double Fourier transform of the function (2.12). First we consider the case $l_f=0$. Then (2.12) reduces to

$$\psi(\underline{r}) \simeq C_f k_f \tfrac{1}{2} i[h_0^{(+)}(k_f r) - e^{-2i\delta_0} h_0^{(-)}(k_f r)] \frac{1}{(4\pi)^{1/2}} , \tag{2.16}$$

where

$$h_0^{(\pm)}(k_f r) = \frac{e^{\pm ik_f r}}{k_f r} .$$

The integral

$$I = \int\int dy\, dz\, e^{-i(yk_y+zk_z)} \frac{e^{\pm ik_f r}}{r} \tag{2.17}$$

is convergent but converges rather slowly. To simplify the discussion we introduce an extra convergence factor $e^{\lambda r}$ with $\lambda>0$ and let $\lambda\to 0$ at the end of the calculation. The integral can be evaluated by the method used by Bonaccorso, Piccolo and Brink[3] by introducing $\gamma = \lambda \mp ik_f$:

$$I = \lim_{\lambda\to 0}\int\int dy\, dz\, e^{-i(yk_y+zk_z)} \frac{e^{-\gamma r}}{r} = -\frac{2\pi}{\gamma_x} e^{-\gamma_x|x|} , \tag{2.18}$$

where

$$\gamma_x = \lim_{\lambda\to 0}(k_y^2+k_z^2+\gamma^2)^{1/2}$$
$$= \lim_{\lambda\to 0}(k_y^2+k_z^2-k_f^2+\lambda^2\mp 2ik_f\lambda)^{1/2}$$
$$= (k_y^2+k_z^2-k_f^2)^{1/2} . \quad (2.19)$$

The interesting point about the above result is that both $h_0^{(\pm)}(kr)$ have the same double Fourier transform so that

$$\bar{\psi}_f(x,k_y,k_z) = -C_f e^{i\delta_0} 2\pi \sin\delta_0 \frac{e^{-\gamma_x|x|}}{\gamma_x}\frac{1}{(4\pi)^{1/2}} . \quad (2.20)$$

This derivation can be easily generalized to the case where $l_f \neq 0$ to give

$$\bar{\psi}_f(x,k_y,k_z) = -C_f e^{i\delta_{l_f}} 2\pi \sin\delta_{l_f} \frac{e^{-\gamma_x|x|}}{\gamma_x} Y_{l_f m_f}(\hat{\mathbf{k}}_f) . \quad (2.21)$$

This has the same form as the double Fourier transform of the bound-state wave function (2.7) where now γ_x is given by Eq. (2.19) rather than Eq. (2.9).

From this point onwards the calculation of the transfer amplitude to a continuum final state can be made in the same way as for the transfer to a final bound state. The final expression for transfer amplitude is the same as Eq. (2.10) with the following replacements.

(a) The normalization constant for the final state

$$C_2 \to C_f e^{i\delta_{l_f}} \sin\delta_{l_f} , \quad (2.22)$$

where the magnitude of C_f is given in Eq. (2.15).

(b) Equation (2.3) for η is replaced by

$$\eta^2 = k_1^2+\gamma_1^2 = k_2^2-k_f^2 . \quad (2.23)$$

(c) Equation (2.11) for the angle β_2 are replaced by

$$\cos\beta_f = \frac{k_2}{k_f}, \quad \sin\beta_f = \frac{i\eta}{k_f} . \quad (2.24)$$

The transfer probability becomes

$$P(l_f,l_i) = \frac{1}{2l_i+1}\sum_{m_1 m_2} |A(l_f,l_i)|^2$$
$$= \frac{\pi}{2}\left(\frac{\hbar}{mv}\right)^2 \frac{2}{L} |\sin\delta_{l_f}|^2 |C_1|^2 (2l_f+1)$$
$$\times P_{l_i}(X_i) P_{l_f}(X_f) \frac{e^{-2\eta R}}{\eta R} , \quad (2.25)$$

where P_{l_i} and P_{l_f} are Legendre polynomials of argument

$$X_i = 1+2\frac{k_1^2}{\gamma_1^2} \text{ and } X_f = 2\frac{k_2^2}{k_f^2}-1$$

and the asymptotic form of the Bessel function has been used

$$K_{m_1-m_2}(\eta R) \approx \left(\frac{\pi}{2\eta R}\right)^{1/2} e^{-\eta R} .$$

Equation (3.3) in Sec. IV gives the transfer probability between bound states. Comparing Eq. (2.25) with Eq. (3.3) we notice that the difference lies in the asymptotic normalization constant of the final state and in the argument of P_{l_2}.

From Eq. (2.25) one can obtain the transfer probability for going to a final state with energy ε_f in a range $d\varepsilon_f$ by introducing the density of final states

$$\rho(\varepsilon_f)d\varepsilon_f = \frac{dn}{d\varepsilon_f}d\varepsilon_f = \frac{L}{\pi}\frac{dk_f}{d\varepsilon_f} = \frac{L}{\pi}\frac{m}{\hbar^2 k_f}d\varepsilon_f , \quad (2.26)$$

where we used the quantization condition

$$k_f L = n\pi$$

which is consistent with the normalization of the final wave function in a box of length L [cf. Eq. (2.15)]. Then

$$\frac{dP}{d\varepsilon_f}(l_f,l_i) = \left(\frac{\hbar}{mv}\right)^2 \frac{m}{\hbar^2 k_f} |\sin\delta_{l_f}|^2 |C_1|^2$$
$$\times (2l_f+1) P_{l_i}(X_i) P_{l_f}(X_f) \frac{e^{-2\eta R}}{\eta R} . \quad (2.27)$$

In Eq. (2.27) the term $\sin\delta_{l_f}$ tends to zero for large l_f, this ensures that the total transfer probability will have contributions only from a limited number of final states with relatively small values of l_f.

If in Eq. (2.12) for the final wave function instead of putting $S_{l_f}^* = e^{-2i\delta_{l_f}}$ one leaves the more general form of the reflexion coefficient S_{l_f} then the transfer probability is written as in Eq. (2.25) but with $|\sin\delta_{l_f}|^2$ substituted by $\frac{1}{4}|1-S_{l_f}|^2$

$$\frac{dP}{d\varepsilon_f}(l_f,l_i) = |1-S_{l_f}|^2 B(l_f,l_i) , \quad (2.28)$$

where

$$B(l_f,l_i) = \frac{1}{4}\left(\frac{\hbar}{mv}\right)^2 \frac{m}{\hbar^2 k_f} |C_1|^2 (2l_f+1)$$
$$\times P_{l_i}(X_i) P_{l_f}(X_f) \frac{e^{-2\eta R}}{\eta R} \quad (2.29)$$

and $B(l_f,l_i)$ can be interpreted as an elementary transition probability. This second form is more suitable for physical interpretation as we shall see later.

Equation (2.27) gives the probability of transfer of a single nucleon in the orbit l_i in the projectile to a continuum state in the target. The discussion in Ref. 4 suggests that when the optimum transfer condition is satisfied ($|Q|_{\text{opt}} = \frac{1}{2}mv^2$) the inclusion of nucleon spin will not alter the result. When there are several neutrons in the orbit l_i the total transfer probability would be obtained by multiplying Eq. (2.27) by the number of active neutrons.

III. TRANSFER TO A SINGLE RESONANCE

The transfer probability formula as given by Eq. (2.27) is appropriate to deal with final states of positive energy

both below and above the centrifugal barrier. Here we discuss states well below the barrier which correspond to narrow resonances. Transfer to these states can be studied by integrating Eq. (2.27) over the energy region of the resonance. By taking a Lorentzian shape for the resonance and assuming that all the other factors in Eq. (2.27) are slowly varying over the resonance we obtain

$$|\sin\delta_{l_f}|^2=\frac{\Gamma}{2}\frac{\Gamma/2}{(\varepsilon-\varepsilon_{\rm res})^2+\Gamma^2/4}\simeq\frac{\Gamma}{2}\pi\delta(\varepsilon-\varepsilon_{\rm res}) \tag{3.1}$$

and

$$\begin{aligned}P(l_f,l_i)&=\int\frac{dP}{d\varepsilon}(l_f,l_i)d\varepsilon\\&\simeq\frac{\Gamma}{2}\pi\int d\varepsilon\,\delta(\varepsilon-\varepsilon_{\rm res})4B(l_{\rm res},l_i)\\&=\frac{\pi}{2}\left[\frac{\hbar}{mv}\right]^2\frac{m\Gamma}{\hbar^2k_{\rm res}}|C_i|^2(2l_f+1)\\&\quad\times P_{l_i}\left[1+2\frac{k_1^2}{\gamma^2}\right]P_{l_f}\left[2\frac{k_2^2}{k_{\rm res}^2}-1\right]\frac{e^{-2\eta R}}{\eta R}\,,\end{aligned} \tag{3.2}$$

where $B(l_{\rm res},l_i)$ is given by Eq. (2.29).

In the case of transfer between bound states [cf. Eq. (3.15) of Ref. 4] the equivalent of Eq. (3.2) was

$$\begin{aligned}P(l_2,l_1)&=\frac{\pi}{2}\left[\frac{\hbar}{mv}\right]^2|C_1C_2|^2(2l_2+1)P_{l_1}\left[1+2\frac{k_1^2}{\gamma_1^2}\right]\\&\quad\times P_{l_2}\left[2\frac{k_2^2}{\gamma_2^2}+1\right]\frac{e^{-2\eta R}}{\eta R}\,.\end{aligned} \tag{3.3}$$

The place of the asymptotic normalization constant of the final state C_2 is then taken by the term $m\Gamma/\hbar^2k_{\rm res}$.

The close resemblance between Eqs. (3.2) and (3.3) suggests that transfer to an isolated resonance can be treated in a very similar way to transfer to a bound state provided one substitute $i\gamma_2$ by $k_{\rm res}$ and $|C_2|^2$ by $m\Gamma/\hbar^2k_{\rm res}$. It seems therefore that the term $m\Gamma/\hbar^2k_{\rm res}$ could be interpreted as an asymptotic normalization constant.

To understand this we use the definition of Γ given in R-matrix theory[14]

$$\Gamma=\frac{\hbar^2k_{\rm res}}{m}\frac{u_l^2(R)}{[k_{\rm res}O_l(k_{\rm res}R)]^2}\,, \tag{3.4}$$

where u_l is the neutron radial wave function calculated in the potential of the target at the resonance energy and $O_l(k_{\rm res}R)=h_l^{(+)}(k_{\rm res}R)$ is its asymptotic form outside a radius R beyond which the nuclear potential vanishes. Then we have

$$\frac{m\Gamma}{\hbar^2k_{\rm res}}=\frac{u_l^2(R)}{[k_{\rm res}O_l(k_{\rm res}R)]^2}\,. \tag{3.5}$$

In the case of transfer to a bound state the asymptotic normalization constant of the final wave function was given by[3]

$$|C_2|^2=\frac{\psi_{\rm num}^2(R)}{[\gamma_2h_l^{(+)}(i\gamma_2R)]^2}\,, \tag{3.6}$$

where $\psi_{\rm num}$ is the numerical solution of the single-particle Schrödinger equation at the experimental binding energy and $h_l^{(+)}(i\gamma_2R)$ is a Hankel function of complex argument imposed as its asymptotic form. C_2 is independent from the radius R when this is taken well outside the nuclear potential.

Therefore we see that when going from negative energies to positive energies, Eq. (3.3) goes smoothly into Eq. (3.2), since Eq. (3.6) goes into Eq. (3.5) provided $u_l(R)$ is normalized inside R, that is

$$\int_0^R u_l^2(r)r^2dr=1\,.$$

In Appendix A we show the correspondence between the normalization of a bound-state wave function and of a resonance wave function in another way which is very close in spirit to the approaches of Vincent[15] and Huby[10] and which gives a formula for the resonance width Γ which does not depend on the choice of the channel radius. Similar results were also obtained in Refs. 11 and 12.

Equation (3.5) is also interesting because at very low energies ($\varepsilon_{\rm res}\to0$) it goes like $k_{\rm res}^{2l}$ and this term will cancel with $P_{l_f}(2k_2^2/k_{\rm res}^2-1)\sim k_{\rm res}^{-2l}$ in Eq. (3.2) so that the transfer probability becomes constant in the limit of zero resonance energy. The same happens in Eq. (3.3) and we expect that the transfer probability calculated from Eq. (3.3) goes smoothly into the one obtained from Eq. (3.2) at zero energy.

IV. TRANSFER TO COMPOUND NUCLEUS STATES

In the derivation of Eq. (2.27) the final state is a single-particle neutron state in the potential of the target. The result depends only on the phase shift δ_{l_f}. This suggests that it might be possible to use Eq. (2.27) when the final state is a compound nucleus state and δ_{l_f} is the exact neutron phase shift including all compound nucleus effects. Equation (3.2) would also hold but Γ would then be a compound nucleus level width rather than a single-particle width.

At energies just above neutron threshold compound nucleus states correspond to narrow resonances. At higher energies the resonances overlap and the neutron cross section becomes smooth. In either case the energy average $\langle S_{l_f}\rangle$ of the elastic S matrix corresponds to the optical model S matrix.[16] If we suppose that in the range of these energy averages only the phase shift changes while $B(l_f,l_i)$ in Eq. (2.29) remains almost constant then the average involves only $|1-S_{l_f}|$ and we get

$$\frac{dP}{d\varepsilon_f}(l_f,l_i)=\langle|1-S_{l_f}|^2\rangle B(l_f,l_i) \tag{4.1}$$

$$=(|1-\langle S_{l_f}\rangle|^2+T_{l_f})B(l_f,l_i)\,, \tag{4.2}$$

where

$$T_{l_f}=1-|\langle S_{l_f}\rangle|^2 \tag{4.3}$$

is the transmission coefficient and $B(l_f,l_i)$ is given by Eq. (2.29).

In Eq. (4.2) the term proportional to $|1-\langle S_{l_f}\rangle|^2$ is due to the shape elastic scattering of the transferred neutron by the target nucleus, while the second term proportional to T_{l_f} is due to compound nucleus formation. Experiments on neutron transfer to continuum states might distinguish between these two components.

Equation (4.2) was obtained under the hypothesis that only the elastic channel was open. In Appendix B the result will be generalized to the case where other channels are open. In that case the transfer probability Eq. (2.28) is replaced by Eq. (B8) in which scattering matrix elements of different channels appear. If we sum over all possible final channels we get Eq. (B10) which depends only on the elastic part S_{00} of the scattering matrix. If S_{00} contains compound nucleus resonances we can average over them and obtain Eq. (B11) which is the same as Eq. (4.2). This result can be understood by a simple physical argument. The transfer probability cannot depend upon which channels are open if the reaction proceeds via compound nucleus formation, because the compound nucleus does not remember via which channel it was formed.

V. CROSS SECTION

In this section we discuss cross sections obtained by applying the theory presented in this paper in connection with the experimental results of Refs. 8 and 18. In Ref. 18 it was pointed out that there is no unique model for nucleon transfer reactions to the continuum which can, at the same time, explain the important features of the experimental energy distributions like the position of the peaks, the widths, and the peak values.

By looking at the experimental spectra contained in Refs. 8 and 18 and at the discussion therein one notices that the transfer cross sections to the continuum are peaked at a final energy close to but always smaller than the incident energy. This suggests that the reaction is of quasielastic nature with almost no excitation of the projectile and that an optimum transfer condition must be satisfied at the peak energy. When the same reaction has been performed at different incident energies it has been seen that the widths increase almost linearly.[8] It is important to have a theory which can predict correctly the position and width of the peak because this information can help to distinguish between the transfer and fragmentation part of inclusive cross sections. This is even more important for multinucleon transfer reactions.

The absolute value of the cross section is more difficult to obtain. From the experimental point of view the problem is that the differential cross sections are known only at certain angles and in order to obtain the total integrated cross sections one has to extrapolate the values to the unknown angles. This procedure can produce errors. From the theoretical point of view the DWBA calculations have an arbitrary normalization and therefore cannot reproduce the yields. Other models can reproduce the yields but only for certain energies and projectile mass (cf. Ref. 18 and references therein).

We now discuss how our model describes the energy dependence of the cross sections. An approximate formula for the total transfer cross section can be obtained from Eq. (4.1) by integrating over impact parameters as in Bonaccorso, Lo Monaco, and Brink[4]

$$\frac{d\sigma}{d\varepsilon_f}=2\pi\int_0^\infty \frac{dP_t}{d\varepsilon_f}P_{el}b\,db$$
$$=\pi\frac{R_s-a_c}{\eta}\frac{dP_t}{d\varepsilon_f}(R_s) \tag{5.1}$$

where

$$\frac{dP_t}{d\varepsilon_f}=\sum_{l_f}\frac{dP}{d\varepsilon_f}(l_f,l_i)\ . \tag{5.2}$$

The nucleus-nucleus probability of elastic scattering P_{el} was given by the sharp cutoff model with strong absorption radius R_s and a_c is the Coulomb length parameter. In Eq. (5.2) $dP(l_f,l_i)/d\varepsilon_f$ is given by Eq. (4.1) with $R=R_s$.

When calculating a spectrum from Eqs. (5.1), (5.2), and (4.1) it is necessary to have the correct behavior of the neutron-nucleus scattering amplitude $\langle S_{l_f}\rangle$. It can be obtained by an optical-model calculation with optical-model parameters depending on the final energy. We use a simple parametrization

$$\langle S_{l_f}\rangle=\frac{1}{1+\exp[(l_g-l_f)/a]}\ , \tag{5.3}$$

where l_g is chosen by the semiclassical approximation $l_g=KR-\frac{1}{2}$. Here R is the radius of the target and K is the neutron-nucleus asymptotic wave number at energy ε_f. We have taken two prescriptions for the diffuseness parameter a. The first is a constant which is independent of energy. The second has an energy dependence given by the prescription $a=l_g/n$ where n is a constant satisfying the condition $l_g\le n$.

Equation (5.1) gives the cross section for transfer between an initial bound state with energy ε_i and angular momentum l_i and a final continuum state with energy ε_f within a range $d\varepsilon_f$. For each energy range we take an incoherent sum over final states as in Eq. (5.2). We define now the total final kinetic energy as

$$E_f=E_{\rm inc}+Q\ , \tag{5.4}$$

where $E_{\rm inc}$ is the initial energy of the projectile in the laboratory, Q is the reaction Q value given by $Q=\varepsilon_i-\varepsilon_f$ where ε_i is the binding energy of the neutron in the last occupied state of the projectile and ε_f is the neutron final energy in the target. The projectile is supposed to remain in its ground state after transfer.

In Figs. 1–4 cross sections per active nucleon $d\sigma/dE_f(=-d\sigma/d\varepsilon_f)$ are shown for several different reactions. The values of the incident energy, the strong absorption radius and the parameters of the initial state are shown in Table I.

Figures 1 and 2 are for the reaction ^{208}Pb(^{16}O,^{15}O)^{209}Pb

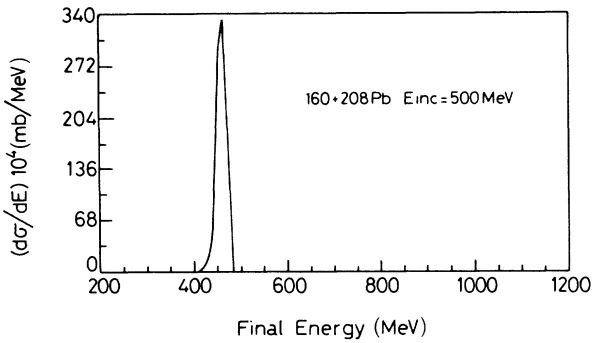

FIG. 1. Spectrum of the reaction ^{208}Pb(^{16}O,^{15}O)^{209}Pb at $E_{\rm inc}=500$ MeV corresponding to values in Table III.

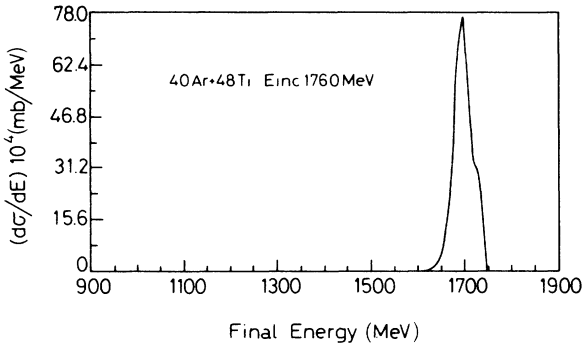

FIG. 3. Spectrum of the reaction ^{48}Ti(^{40}Ar,^{39}Ar)^{49}Ti at $E_{\rm inc}=1760$ MeV corresponding to values in Table III.

at 500 MeV and 800 MeV, respectively. Figure 3 is for the reaction ^{48}Ti(^{40}Ar,^{39}Ar)^{49}Ti at 1760 MeV which has been described in Ref. 21. Figure 4 is for the reaction ^{197}Au(^{20}Ne,^{19}Fl)^{198}Hg at 341 MeV which has been studied experimentally by Wald *et al.*[18]

The results in Figs. 1–3 are for neutron transfer and are calculated with a diffuseness parameter a given by the energy-dependent prescription $a=l_g/n$. Figure 4 shows an example for proton transfer and the diffuseness parameter is fixed at $a=0.65$. The dependence on the choice of a can be seen by comparing the results in Tables II and III.

The characteristics of the spectra shown in Figs. 1–4 are summarized in Tables II and III, where $E_{\rm inc}$ is the projectile incident energy in the laboratory, $\frac{1}{2}mv^2$ is the incident energy per nucleon at the instant of transfer, $E_{\rm mean}/A_1$ is the value of the projectile final energy [Eq. (5.4)] at which the peak of the cross section occurs divided by the number of the nucleons in the projectile. The optimum transfer condition discussed later corresponds to $E_{\rm mean}/A_1\simeq\frac{1}{2}mv^2$. The fourth columns in Tables II and III show the widths of the cross sections taken at half the peak value and the last columns show the peak value multiplied by a factor 10^4.

First one notices that the positions of the peaks correspond to a final energy

$$E_f\simeq E_{\rm inc}+Q_{\rm opt} \tag{5.5}$$

where

$$|Q_{\rm opt}|=|\varepsilon_i-\varepsilon_f|=\tfrac{1}{2}mv^2 \tag{5.6}$$

and v is the relative velocity at the point of transfer. This can be seen for example by comparing the values of $E_{\rm mean}/A_1$ with $\frac{1}{2}mv^2$ in Table II.

This feature of the quasielastic reactions to prefer a final state with the target excited has already been noticed by other authors.[8] In our formalism it is clear why and how it happens: The transfer probability and cross section as given by Eqs. (4.1) and (5.1) have a maximum when the parameter η has a minimum and from Eqs. (2.3) and (2.5) this happens when $|Q|=|Q_{\rm opt}|=\frac{1}{2}mv^2$. Therefore the most favored final energy of the target is $\varepsilon_f=\varepsilon_i+\frac{1}{2}mv^2$ with $\varepsilon_f>0$ since $\frac{1}{2}mv^2\geq|\varepsilon_i|$ at the incident energies we are concerned with ($E_{\rm inc}$/nucleon$=20\div100$ MeV). The reaction proceeds via transfer of the nucleon to a continuum state of the target having final energy equal to the initial binding energy plus the energy per nucleon of relative motion.

In Tables II and III one notices that the widths of the peaks in the transfer cross section increase with the incident energy. The increase in widths is almost linear with incident energies, typical values are between 20 and

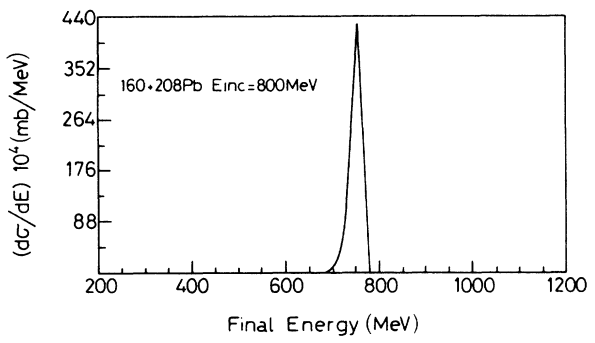

FIG. 2. Spectrum of the reaction ^{208}Pb(^{16}O,^{15}O)^{209}Pb at $E_{\rm inc}=800$ MeV corresponding to values in Table III.

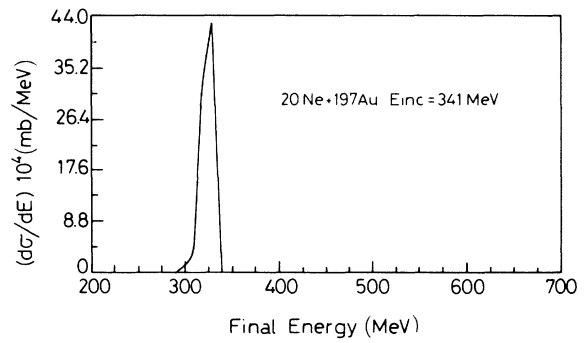

FIG. 4. Spectrum of the reaction ^{197}Au(^{20}Ne,^{19}Fl)^{198}Hg at $E_{\rm inc}=341$ MeV corresponding to values in Table II.

TABLE I. Parameters used in the numerical calculations.

Reaction	E_{inc} (MeV)	R_s (fm)	ε_i (MeV)	C_i (fm$^{-1/2}$)	l_i
^{208}Pb(^{16}O,^{15}O)^{209}Pb	312.6	11.96	−15.664	7.28	1
	500	11.75			
	800	11.52			
	1100	11.40			
^{48}Ti(^{40}Ar,^{39}Ar)^{49}Ti	1760	9.87	−9.871	2.62	3
^{197}Au(^{20}Ne,^{19}Fl)^{198}Hg	341	11.95	−12.845	6.5	2

TABLE II. Characteristics of some spectra calculated with $a=0.65$ where a is defined in Eq. (5.3).

Reaction	E_{inc} (MeV)	$\frac{1}{2}mv^2$ (MeV)	$\frac{E_{mean}}{A_1}$ (MeV)	Width (MeV)	$\sigma(E_f)_{peak}\times 10^4$ (mb/MeV)
^{208}Pb(^{16}O,^{15}O)^{209}Pb	312.6	14.22	19	17	59
	500	25.84	29	25	142
	800	44.48	47	37	152
	1100	63.17	64	59	110
^{48}Ti(^{40}Ar,^{39}Ar)^{49}Ti	1760	41.35	43	44	52
^{197}Au(^{20}Ne,^{19}Fl)^{198}Hg	341	11.81	16	18	43

TABLE III. The same as Table II but $a=l_g/12$ for $l_g\leq 12$, $a=0.8$ for $l_g>12$.

Reaction	E_{inc} (MeV)	$\frac{1}{2}mv^2$ (MeV)	$\frac{E_{mean}}{A_1}$ (MeV)	Width (MeV)	$\sigma(E_f)_{peak}\times 10^4$ (mb/MeV)
^{208}Pb(^{16}O,^{15}O)^{209}Pb	312.6	14.22	19	23	106
	500	25.84	29	26	337
	800	44.48	47	31	425
	1100	63.17	64	43	328
^{48}Ti(^{40}Ar,^{39}Ar)^{49}Ti	1760	41.35	43	42	77
^{197}Au(^{20}Ne,^{19}Fl)^{198}Hg	341	11.81	16	25	80

TABLE IV. Variation as a function of the final energy ε_f of the parameters and factors appearing in Eq. (5.7) for the reaction ^{208}Pb(^{16}O,^{15}O)^{209}Pb at $E_{inc}=800$ MeV discussed also in Table III. The last column shows the cross section per active nucleon.

ε_f (MeV)	η (fm^{-1})	l_g	$P_{l_i}\left[1+2\frac{k_1^2}{\gamma^2}\right]$	$S(l_g)$	$F(\eta)$ (fm^2)	$\sigma(\varepsilon_f)\times 10^4$ (mb/MeV)
10	0.922	4	1.25	1.62×10^6	5.44×10^{-11}	90.1
30	0.869	8	1.00	4.31×10^6	9.66×10^{-11}	424
50	0.936	10	1.32	8.96×10^6	1.81×10^{-11}	166
70	1.102	12	2.22	9.81×10^7	4.07×10^{-13}	39.1
90	1.329	14	3.68	2.49×10^9	2.14×10^{-15}	5.45
110	1.593	15	5.73	1.02×10^{11}	4.82×10^{-18}	0.50
130	1.878	17	8.35	6.42×10^{12}	6.62×10^{-21}	0.043
150	2.175	18	11.5	3.91×10^{14}	6.76×10^{-24}	0.0027

TABLE V. Contribution from different initial states to the total cross section which is shown in the last column. The second column contains the values of the cross section per active nucleon. The reaction is ^{208}Pb(^{16}O,^{15}O)^{209}Pb at $E_{inc}=800$ MeV discussed also in Table II.

Initial State	$\sigma(E_f)_{peak}\times 10^4$ (mb/MeV)	Active neutrons	$\sigma_T(E_f)_{peak}\times 10^4$ (mb/MeV)
$1p_{1/2}$	152	2	306
$1p_{3/2}$	76	4	306
$1s_{1/2}$	59	2	117

60 MeV in agreement with experimental results.[8]

The peak cross section for the first reaction varies with incident energy and has a maximum for $E_{\rm inc}=800$ MeV. The values of the peak cross section are very sensitive to the choice of the strong absorption radius and to the diffuseness parameter a in the neutron optical model amplitude Eq. (5.3). A comparison of the results in Tables II and III shows that the peak cross section is about a factor 3 larger when the energy dependent diffuseness is used rather than the fixed one.

Table IV shows an example of the contributions of different terms in Eq. (5.1) which can be written as

$$\frac{d\sigma}{d\varepsilon_f}=\frac{\pi}{4}(R_s-a_c)\,|\,C_i\,|^2\left[\frac{2}{mv^2}\right]S(l_f)F(\eta)\ , \qquad (5.7)$$

where

$$S(l_f)=\sum_{l_f}(\,|\,1-\langle S_{l_f}\rangle\,|^2+T_{l_f})(2l_f+1)P_{l_f}\left[2\frac{k_2^2}{k_f^2}-1\right] \qquad (5.8)$$

and

$$F(\eta)=P_{l_i}\left[2\frac{k_1^2}{\gamma^2}+1\right]\frac{e^{-2\eta R_s}}{2\eta R_s k_f\eta}\ . \qquad (5.9)$$

The term $P_{l_i}(2k_1^2/\gamma^2+1)$ contains the contribution to the energy dependence coming from the initial state. This term increases with energy but it does not change so much. The term $S(l_f)$ contains most of the information from the final state. There is a very strong increase with final energy. This is mainly because l_f becomes bigger so that more terms contribute. The term $P_{l_f}(2k_2^2/k_f^2-1)$ can became very large when l_f is large. $S(l_f)$ is very sensitive to the choice of l_g and a because the optical-model factor determines the cutoff of high l_f contributions. The term $F(\eta)$ is very sensitive to the value of η and has a maximum when η has a minimum. It decreases very rapidly at high energy because of the increase in the value of η. The peak in the spectrum in Fig. 2 corresponds to a situation where $\eta\approx\gamma$, $k_1\approx 0$. The energy dependence of the various terms shown in Table IV is typical of this kind of reaction.

We would now like to discuss how our formalism can be used to predict or discuss experimental results. Our estimates for the position of the peaks and for the widths are in qualitatitive agreement with the trends of the experimental results reported in Refs. 8 and 18. Also our calculations do not have an arbitrary normalization like the DWBA calculations of Mermaz,[7] therefore they should in principle be able to predict the yields of the reactions. However, to get reasonable estimates of the yields the results from Eq. (5.1) which gives the cross section per active neutron in the level l_i should be multiplied by the number of active neutrons in the orbit and transitions from all occupied orbits in the projectile should be included. To show the importance of such modifications we have calculated the cross section Eq. (5.1) for the reaction ^{208}Pb(^{16}O,^{15}O)^{209}Pb at $E_{\rm inc}=800$ MeV, with the bound-state parameters of Ref. 4, and with a constant diffuseness of $a=0.65$ in Eq. (5.3). Table V shows the peak values of $\sigma(E_f)$ for all possible initial states in oxygen. The results in column 2 come from Eq. (5.1) while those in column 4 are obtained multiplying the cross section per active neutron by the number of active neutrons in the orbit. The total peak value of $\sigma_T(E_f)$ becomes 729×10^{-4} mb/MeV while taking into account only the last occupied orbit in oxygen we obtained a peak cross section per active nucleon equal to 152.1×10^{-4} mb/MeV. Therefore it is important to take into account all possible initial states if one is interested in predicting the yields of a reaction, while the position of the peak and the width are well reproduced by taking into account only the last occupied orbit.

One nice point about our procedure is the extremely short CPU time necessary to calculate one spectrum. It takes between four and five seconds and this includes the time used to run library routines which give a plot of the spectrum. We have used the VAX 11/780 computer of the Department of Physics in Catania.

Proton transfer can be calculated from the formulae given in this paper by using effective binding energies, Q values and normalization constants. Figure 4 shows an example of our results obtained using the effective values discussed in Lo Monaco.[17] Lo Monaco uses the following prescription for transfer between bound states: The effective Q values is given by

$$Q_{\rm eff}=\varepsilon_i-\varepsilon_f-[V_1^c(d_1)-V_2^c(d_2)]=\bar{\varepsilon}_1-\bar{\varepsilon}_2\ ,$$

where $\bar{\varepsilon}_1$ and $\bar{\varepsilon}_2$ are effective binding energies defined by

$$\bar{\varepsilon}_\alpha=\varepsilon_\alpha-\frac{z_{c_\alpha}e^2}{d_\alpha},\quad \alpha=1,2$$

and

$$V_\alpha^c(d_\alpha)=\frac{z_{c_\alpha}e^2}{d_\alpha}$$

is the Coulomb potential between the proton and the core in the initial and final nucleus, respectively, taken at the point d_α where

$$\frac{d_1}{d_2}=\frac{A_1^{1/3}}{A_2^{1/3}}\ \text{and}\ d_1+d_2=R_s\ .$$

$A_{1,2}$ are the mass numbers of projectile and target respectively and R_s is the strong absorption radius.

The effective normalization constant for the initial bound state is obtained from Eq. (3.6) calculated at $R=R_s$ and $\bar{\gamma}^2=-2m\bar{\varepsilon}_1/\hbar^2$.

For the proton transfer between ^{20}Ne and ^{197}Au at $E_{\rm inc}=341$ MeV, shown in Fig. 4 we get a width of 25 MeV in very good agreement with the value of 26 MeV given by Wald *et al.*[18] for the transfer part of their inclusive spectrum at the grazing angle.

The use of effective parameters as discussed here corresponds to a sudden approximation for the effect of the Coulomb field of the other nucleus in proton transfer. Hashim and Brink (private communication) have shown that the use of another set of parameters corresponding

to an adiabatic approximation does not affect the results very much.

VI. CONCLUSIONS

In this paper we have derived an analytical formula for the calculation of energy spectra for one nucleon transfer to the continuum. The normalization of final unbound states is determined automatically by the theory and it is an agreement with other results[9,10,15] obtained from more sophisticated scattering theories. Both isolated and overlapping resonances can be discussed.

The transfer probability formula has the structure of an elementary transfer probability weighted by the sum of the compound nucleus formation probability plus the probability of nucleon elastic scattering by the target as given by the optical model.

Calculated spectra show general trends in agreement with experimental data. The peaks correspond to an optimum Q value whose definition is given by the theory as $|Q_{\rm opt}|=\frac{1}{2}mv^2$, where $\frac{1}{2}mv^2$ is the relative energy per nucleon at the instant of transfer. Widths are between 20 and 60 MeV and they increase almost linearly with the incident energy.

We think that this method can be used for the prediction of transfer cross section at higher energies than those presently available and might be reliable for the separation of transfer components from breakup components of inclusive spectra.

ACKNOWLEDGMENTS

We are very grateful to M. Di Toro for his interest in the early stages of this work. We would also like to thank R. Huby for discussions which helped us to understand the relation between our work and other theories of transfer to continuum states. We also acknowledge the help of C. Santagati in checking some calculations and running our programs. One of us (A.B.) thanks the Department of Theoretical Physics in Oxford for the very warm hospitality on several occasions during the preparation of this paper.

APPENDIX A

In this appendix we show the correspondence between the asymptotic normalization constant of a bound-state wave function and the normalization of a resonance wave function. Vincent[15] and Huby[10] have shown that the normalization of a resonance wave function depends upon the width Γ and they have obtained a formula for Γ. We obtain the same result as Refs. 10 and 15 following a different method.

In the case of a bound state the wave function is

$$\psi_l(\underline{r})=C\frac{\chi(r)}{r}Y_{lm}(\theta,\varphi)\ , \tag{A1}$$

where $\chi(r)$ is a solution of the Schrödinger equation

$$\frac{d^2\chi}{dr^2}-\gamma^2\chi=\frac{2m}{\hbar^2}V(r)\chi \tag{A2}$$

with boundary condition $\chi(0)=0$. Outside the range of the nuclear potential

$$\chi(r)=\chi_{\rm ext}(r)=-i^l\gamma r h_l^{(1)}(i\gamma r),\quad r>R \tag{A3}$$

at the bound state energy $\varepsilon=-\gamma^2$. The normalization constant C in Eq. (A1) is obtained from

$$C^2\int_0^\infty\chi^2(r)dr=1$$

so that

$$C^2=\left[\int_0^\infty\chi^2(r)dr\right]^{-1}\ . \tag{A4}$$

An alternative formula for C^2 can be obtained from the Wronskian propriety (Ref. 19, Eq. III-28) which holds when $\chi(a)$ and $\chi'(a)$ have fixed values

$$\chi^2(b)\frac{\partial}{\partial\varepsilon}\left[\frac{1}{\chi}\frac{\partial\chi}{\partial r}\right]_b=\int_b^a\chi^2(r)dr\ . \tag{A5}$$

One can take the limit $a\to\infty$ if $\chi\to0$ as $r\to\infty$. Using Eq. (A3) we obtain

$$\int_R^\infty\chi_{\rm ext}^2(r)dr=\chi_{\rm ext}^2(R)\frac{\partial}{\partial\varepsilon}\left[\frac{1}{\chi_{\rm ext}}\frac{\partial\chi_{\rm ext}}{\partial r}\right]_R$$
$$=\frac{1}{2\gamma}F(\gamma R)\ , \tag{A6}$$

where

$$F(\rho)=\chi^2(R)\frac{d}{d\rho}\left[\frac{1}{h_l^{(1)}(i\rho)}\frac{d}{d\rho}\rho h_l^{(1)}(i\rho)\right] \tag{A7}$$

substituting Eq. (A6) in Eq. (A4)

$$C^2=\left[\int_0^R\chi^2(r)dr+\frac{1}{2\gamma}F(\gamma R)\right]^{-1}\ . \tag{A8}$$

In the case of an unbound state the wave function is still of the form (A1) with $-\gamma^2$ substituted by $k^2=\varepsilon$ and with the boundary condition $\chi(0)=0$. Outside the range of the nuclear potential Eq. (A3) is replaced by

$$\chi_{\rm ext}(r)\simeq kr[\cos\delta j_l(kr)+\sin\delta n_l(kr)],\quad r>R \tag{A9}$$

where j_l and n_l are the regular and irregular Bessel functions defined in Ref. 19, p. 415. Equation (A9) holds at any energy $\varepsilon=k^2$. It reduces to

$$\chi_{\rm ext}(r,\varepsilon_0)=k_0 r n_l(k_0 r) \tag{A10}$$

at resonance energy $\varepsilon_0=k_0^2$, since in that case $\cos\delta=0$ and $\sin\delta=1$. Near resonance Eq. (A9) can be written as

$$\chi_{\rm ext}(r,\varepsilon)=k_0 r n_l(kr)+k_0 r A(\varepsilon)j_l(kr) \tag{A11}$$

where

$$A(\varepsilon)=\frac{2(\varepsilon_0-\varepsilon)}{\Gamma}\ .$$

Near a resonance one can use Eq. (A5) with $a=0$ since $\chi(0)=0$. The left-hand side of Eq. (A5) can be written as

$$\chi^2(R)\frac{\partial}{\partial\varepsilon}\left[\frac{1}{\chi}\frac{\partial\chi}{\partial r}\right]_R=\frac{\chi^2(R)}{2k}\frac{\partial}{\partial k}\left[\frac{1}{\chi}\frac{\partial\chi}{\partial r}\right]_R$$
$$=\frac{1}{2k_0}\left[\chi\left[\frac{\partial^2\chi}{\partial k\partial r}\right]_{k_0}-\left[\frac{\partial\chi}{\partial k}\right]_{k_0}\frac{\partial\chi}{\partial r}\right]_R$$
$$=\frac{1}{2k_0}G(k_0R)-\frac{\hbar^2k_0}{m\Gamma}\ , \tag{A12}$$

where

$$G(\rho)=\chi^2(R)\frac{d}{d\rho}\left[\frac{1}{n_l}\frac{d}{d\rho}\rho n_l(\rho)\right] \tag{A13}$$

and Eq. (A5) reduces to

$$-\int_0^R\chi^2(r)dr=\frac{1}{2k_0}G(k_0R)-\frac{\hbar^2k_0}{m\Gamma}\ .$$

It follows that

$$\frac{m\Gamma}{\hbar^2k_0}=\left[\int_0^R\chi^2(r)dr+\frac{G(k_0R)}{2k_0}\right]^{-1}\ . \tag{A14}$$

Equation (A14) was already obtained by Vincent.[15] The close resemblance between Eqs. (A8) and (A14) suggests that the term $m\Gamma/\hbar^2k_0$ can be interpreted as the normalization constant of a resonance wave function. It is interesting to note that Eq. (A14) is independent of the choice of R provided R is taken outside the nuclear potential.

APPENDIX B

In this appendix we generalize the results of Sec. II to the case in which the initial and final channels are many particle states. We need to generalize the wave functions in Eq. (2.1). We consider a case in which the core of the projectile has no structure and zero spin and always remains in its ground state. In the initial state the neutron is in the projectile in a bound state $\phi_1(\underline{r})$ and the target is in its ground state $\chi_0(\xi)$ which has zero spin. The ξ are the internal coordinates of the target. The neutron is transferred to a continuum state in the target and its final state is $\Psi_a(\underline{r},\xi)$ satisfying a boundary condition with a neutron in an outgoing wave state $\phi_a^{(+)}(\underline{r})$ and the target in an excited state $\chi_a(\xi)$. We need the initial and final states only on the surface Σ discussed in Sec. II and on that surface they can be approximated by their asymptotic forms. The appropriate asymptotic form of $\Psi_a(\underline{r},\xi)$ is the antiscattering state

$$\Psi_a(\underline{r},\xi)=C_a\left[\phi_a^{(+)}(\underline{r})\chi_a(\xi)-\sum_b S_{ba}^*\phi_b^{(-)}(\underline{r})\chi_b(\xi)\right] \tag{B1}$$

where $\phi_\alpha^{(\pm)}(\underline{r})$, with $\alpha=a,b$ are the outgoing and incoming scattering waves. The S_{ba}^* are S-matrix elements for the antiscattering of a neutron by the target.

On the surface Σ we can use the asymptotic form for the $\phi_\alpha^{(\pm)}$ in terms of Hankel functions

$$\phi_\alpha^{(\pm)}(\underline{r})\simeq(v_\alpha)^{-1/2}k_\alpha h_l^{(\pm)}(k_\alpha,r)Y_{lm}(\hat{\mathbf{r}})\ . \tag{B2}$$

The term $(v_\alpha)^{-1/2}$ appears because of the condition $v_a(\phi_a^{(+)*}\phi_a^{(+)})r^2=1$, which imposes unit outgoing flux in the exit channel. With this normalization the scattering matrix elements satisfy the unitary condition

$$\sum_b S_{ba}^*S_{ba'}=\delta_{aa'}\ . \tag{B3}$$

According to Blatt and Weisskopf[20] (p. 523) the normalization constant C_a in Eq. (B1) is given by

$$|C_a|^2=\frac{1}{2T}\ , \tag{B4}$$

where

$$T=\frac{L_b}{v_b}=\frac{L_a}{v_a}$$

and

$$\frac{|C_a|^2}{v_a}=\frac{C_f^2}{4}=N^2\ ,$$

where C_f and N are defined in Eq. (2.15).

Their argument proceeds in terms of wave trains. They say that the time over which the waves are active must be the same in all channels (and the same as the time over which the incoming wave was switched on) and since they travel with different velocities in each channel, then they must be normalized in boxes of different length.

The density of final neutron states can also be defined in terms of T by

$$\rho(\varepsilon)d\varepsilon=\frac{T}{2\pi\hbar}d\varepsilon\ . \tag{B5}$$

The Fourier transforms of (B2) can be defined and calculated as in Sec. II giving $\bar{\phi}_\alpha^{\pm}(d_2,k_y,k_2)$, and $\bar{\phi}_1(d_1,k_y,k_1)$ will be the Fourier transform of the initial neutron state.

The transfer amplitude will be

$$A_a=\frac{i\hbar C_a}{2m\pi v}\int dk_y(\eta^2+k_y^2)^{1/2}\times[\delta_{0a}\bar{\phi}_a^{(+)*}\bar{\phi}_1-S_{0a}\bar{\phi}_0^{(-)*}\bar{\phi}_1]\ , \tag{B6}$$

where v is the velocity of relative motion at the instant of transfer, η and $k_{1,2}$ are defined in Eqs. (2.23) and (2.5).

Equation (B6) contains δ_{0a} as a result of the intergration over the internal variables ξ which gives

$$\int\chi_a^*(\xi)\chi_b(\xi)d\xi=\delta_{ab}\ . \tag{B7}$$

From now on the calculation procedes as in Sec. II since the $\bar{\phi}$ are the Fourier transforms of the neutron initial and final wave functions.

The transfer probability to a final state where the target is left in an excited state $\chi_a(\xi)$ with excitation energy ε_a and the final neutron has an energy $\varepsilon-\varepsilon_a$ relative to the target is

$$\frac{dP_a}{d\varepsilon}=|\delta_{0a}-S_{0a}|^2B(l_f,l_i)\ . \tag{B8}$$

Summing over all final states of the target gives

$$\frac{dP}{d\varepsilon} = \left[|1-S_{00}|^2 + \sum_{a\neq 0} |S_{0a}|^2 \right] B(l_f,l_i) , \quad \text{(B9)}$$

where $B(l_f,l_i)$ is given by Eq. (2.29) of the text and l_i,l_f are the orbital angular momenta belonging to the set of quantum numbers which characterize the initial and final states respectively.

Equation (B8) is the generalization of Eq. (2.28) to include the effect of excitation of the target by the transferred neutron. By using the unitarity property of the S matrix Eq. (B9) can also be written as

$$\frac{dP}{d\varepsilon} = (|1-S_{00}(\varepsilon)|^2 + 1 - |S_{00}(\varepsilon)|^2) B(l_f,l_i) \quad \text{(B10)}$$

in this equation ε is the energy of the neutron relative to the target and $S_{00}(\varepsilon)$ is the S-matrix element for elastic scattering of a neutron with energy ε by the target.

The S-matrix element $S_{00}(\varepsilon)$ may have resonances corresponding to compound states made up of target plus neutron states. Average of these resonances gives

$$\frac{dP}{d\varepsilon} = (|1-\langle S_{00}\rangle|^2 + 1 - |\langle S_{00}\rangle|^2) B(l_f,l_i) \quad \text{(B11)}$$

which is the same as Eq. (4.2) of the text.

[1] L. Lo Monaco and D. M. Brink, J. Phys. G **11**, 935 (1985).
[2] Fl. Stancu and D. M. Brink, Phys. Rev. C **32**, 1937 (1985).
[3] A. Bonaccorso, G. Piccolo, and D. M. Brink, Nucl. Phys. **A441**, 555 (1985).
[4] A. Bonaccorso, D. M. Brink, and L. Lo Monaco, J. Phys. G **13**, 1407 (1987).
[5] H. Hashim and D. M. Brink, Nucl. Phys. **A476**, 107 (1988).
[6] T. Tamura and T. Udagawa, Phys. Lett. **71B**, 273 (1977).
[7] M. C. Mermaz, Phys. Lett. **155B**, 330 (1985).
[8] M. C. Mermaz, V. Borrel, D. Guerrean, J. Galin, B. Gatty, and D. Jacquet, Z. Phys. A **324**, 217 (1986).
[9] D. Kelvin and R. Huby, J. Phys. G **3**, 239 (1977).
[10] R. Huby, J. Phys. G **11**, 921 (1985), and references therein.
[11] G. Baur and D. Trautmann, Phys. Rep. **25C**, 293 (1976); Z. Phys. **267**, 103 (1974).
[12] R. Lipperheide and K. Möhring, Nucl. Phys. **A211**, 125 (1973); R. Lipperheide, Phys. Lett. **32B**, 555 (1970).
[13] K. W. McVoy and M. C. Nemes, Z. Phys. A **295**, 177 (1980).
[14] A. M. Lane, R. G. Thomas, and E. P. Wigner, Phys. Rev. **98**, 639 (1955).
[15] C. M. Vincent, Nucl. Phys. **A113**, 249 (1968).
[16] H. Feshbach, C. E. Porter, and V. F. Weisskopf, Phys. Rev. **96**, 448 (1954).
[17] L. Lo Monaco, Ph. D. thesis, University of Oxford, 1985.
[18] S. Wald, S. B. Gazes, C. R. Albiston, Y. Chan. B. G. Harvey, M. J. Murphy, I. Tserruya, R. G. Stokstad, P. J. Countryman, K. Van Bibber, and H. Homeyer, Phys. Rev. C **32**, 894 (1985).
[19] A. Messiah, *Mécanique Quantique* (Dunot, Paris, 1958), Vol. 1.
[20] J. M. Blatt and V. F. Weisskopf, *Theoretical Nuclear Physics* (Springer-Verlag, Berlin, 1979), p. 523.
[21] M. C. Mermaz, R. Dayras, J. Barrette, B. Berthier, D. M. De Castro Rizzo, O. Cisse, R. Legrain, A. Pagano, P. Pollacco, H. Delagrange, W. Mittig, B. Heusch, G. Lanzanò, and A. Palmeri, Nucl. Phys. **A441**, 129 (1985).